

Supplementary information for

Condensation of 9-fluorenone and phenol using the ionic liquid and mercapto compound synergistic catalyst

Lei Yan^{a,b}, Limei Yu^{*a,b}, Maochang Shen, Shikang Luo and Zhanxian Gao^b

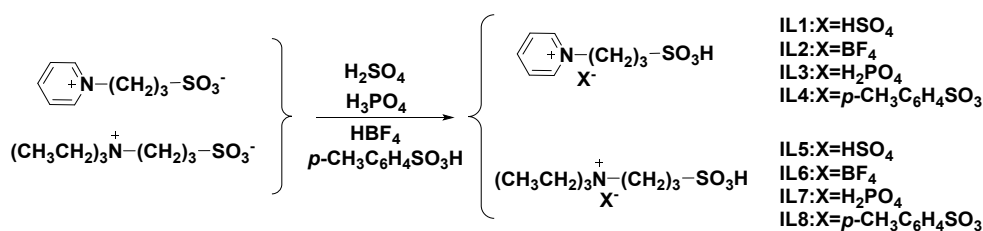
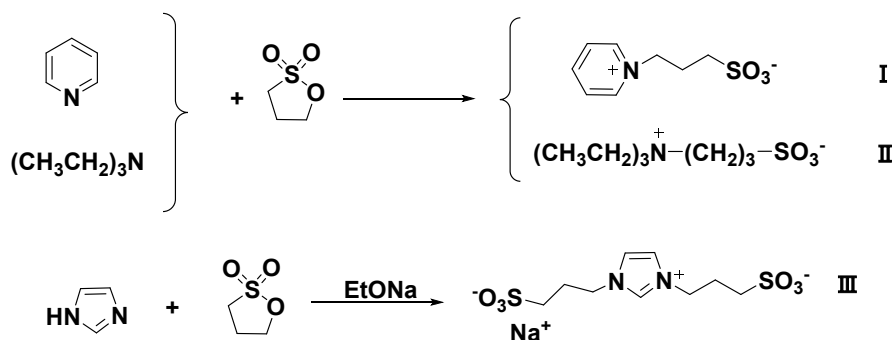
^a State Key Lab of Fine Chemicals, Dalian University of Technology, Dalian, Liaoning 116024, China.

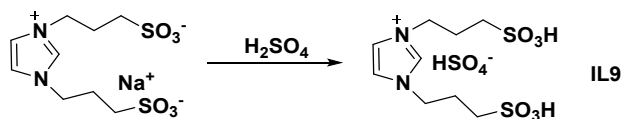
^b School of Chemical Engineering, Dalian University of Technology, Dalian, Liaoning 116024, China

*To whom correspondence should be addressed. Email: ochem@dlut.edu.cn

1. Characterization

Fourier transform infrared (FT-IR) spectra in the frequency range of 4000–400 cm⁻¹ were recorded on a Nicolet 460 spectrometer (Nicolet, USA) using KBr pellets and liquid membrane method. ¹H and ¹³C NMR spectra were recorded on a Bruker Avance II 400 MHz with TMS as an internal standard. The ESI-MS data of IL1~3 and IL5~7 were recorded on a MS (Q-TOF Micro) at the mode of positive and negative. The data of thermal stability for the ILs were obtained by TGA (Shimadzu TGA-50) at a heating rate of 10 K / min under nitrogen.





Scheme 2 The synthetic of ionic liquids

1.1 Structural characterization of Precursors (I, II and III)

Spectral data for (I): ^1H NMR (400 MHz, D_2O , TMS) δ (ppm): 8.79 – 8.68 (d, $J = 6.1$ Hz, 2H), 8.41 (t, $J = 7.8$, 1.4 Hz, 1H), 7.99 – 7.82 (t, $J = 7.0$ Hz, 2H), 4.63 (t, $J = 7.4$ Hz, 2H), 2.91 – 2.68 (m, 2H), 2.32 (m, 2H). ^{13}C NMR (400 MHz, D_2O , TMS) δ (ppm): 146.01, 144.51, 128.50, 60.00, 47.21, 26.30. FI-IR (KBr, v/cm^{-1}): 3028, 2954, 1628, 1500, 1486, 1469, 1324, 1237, 1161, 1056.

Spectral data for (II): ^1H NMR (400 MHz, D_2O , TMS) δ (ppm): 3.29 – 3.24 (t, $J = 9.2$ Hz, 2H), 3.24 – 3.18 (m, 6H), 2.88 (t, $J = 7.0$ Hz, 2H), 2.10 – 1.98 (m, 2H), 1.19 (t, $J = 7.4$ Hz, 9H). ^{13}C NMR (400MHz, D_2O , TMS) δ (ppm): 54.72, 52.65, 47.24, 17.23, 6.60. FI-IR (KBr, v/cm^{-1}): 2991, 2957, 1460, 1380, 1155, 1036.

Spectral data for (III): ^1H NMR (400 MHz, D_2O , TMS) δ (ppm) 8.82 (s, 1H), 7.53 (d, $J = 1.7$ Hz, 2H), 4.33 (t, $J = 7.2$ Hz, 4H), 2.96 – 2.78 (t, $J = 8.0$, 4H), 2.28 (m, 4H). ^{13}C NMR (400MHz, D_2O , TMS) δ (ppm): 135.80, 122.62, 47.93, 47.30, 25.07. FI-IR (KBr, v/cm^{-1}): 3035, 2940, 1595, 1490, 1460, 1342, 1154, 1064.

1.2 Structural characterization of ionic liquids (IL1-IL9)

Spectral data for IL1: ^1H NMR (400MHz, D_2O , TMS) δ (ppm): 8.59 – 8.51 (d, $J = 6.2$ Hz, 2H), 8.25 (t, $J = 7.8$, 1.4 Hz, 1H), 7.84 – 7.68 (t, $J = 7.0$ Hz 2H), 4.45 (t, $J = 7.5$ Hz, 2H), 2.66 (t, $J = 8.0$, 6.7 Hz, 2H), 2.14 (m, 2H). ^{13}C NMR (400 MHz, D_2O , TMS) δ (ppm): 145.79, 144.19, 128.27, 59.70, 46.90, 25.95. FI-IR (v/cm^{-1}): 3250, 3068, 2969, 1636, 1492, 1460, 1237, 1160, 1056. ESI-MS Positive Mass Peaks (m/z): 202.13, 403.21; ESI-MS Negative Mass Peaks (m/z): 96.98. TG (N_2 , 10°C min^{-1}): $T_d = 348^\circ\text{C}$.

Spectral data for IL2: ^1H NMR (400MHz, D_2O , TMS) δ (ppm): 8.77 (d, $J = 6.1$ Hz, 2H), 8.46 (t, $J = 7.9$ Hz, 1H), 7.98 (t, $J = 7.0$ Hz, 2H), 4.67 (t, $J = 7.5$ Hz, 2H), 2.88 (t, $J = 7.3$ Hz, 2H), 2.36 (m, 2H). ^{13}C NMR (400MHz, D_2O , TMS) δ (ppm): 145.93, 144.38, 128.41, 59.89, 47.05, 26.11. FI-IR (v/cm^{-1}): 3285, 3075, 2972, 1663, 1494, 1321, 1291, 1172, 1087. ESI-MS Positive Mass Peaks (m/z): 202.13, 403.12, 604.33; ESI-MS Negative Mass Peaks (m/z): 87.03. TG (N_2 , 10°C min^{-1}): $T_d = 350^\circ\text{C}$.

Spectral data for IL3: ^1H NMR (400MHz, D_2O , TMS) δ (ppm): 8.75 (d, $J = 6.1$ Hz, 2H), 8.43 (t, $J = 7.9$, 1.3 Hz, 1H), 7.96 (t, $J = 7.0$ Hz, 2H), 4.64 (t, $J = 7.4$ Hz, 2H),

2.85 (t, $J = 7.3$ Hz, 2H), 2.33 (m, 2H).¹³C NMR (400MHz, D₂O, TMS) δ (ppm): 145.89, 144.34, 128.38, 59.85, 47.01, 26.08. FI-IR (v/cm⁻¹): 3216, 3069, 2971, 1630, 1491, 1208, 1124, 973. ESI-MS Positive Mass Peaks (m/z): 202.12, 403. 21, 604.34; ESI-MS Negative Mass Peaks (m/z): 97.01. TG (N₂, 10 °C min⁻¹): T_d = 339°C.

Spectral data for IL4: ¹H NMR(400MHz, D₂O, TMS) δ (ppm): 8.72 (d, $J = 6.0$ Hz, 2H), 8.40 (t, $J = 7.8$ Hz, 1H), 7.93 (t, $J = 7.0$ Hz, 2H), 7.54 (d, $J = 8.0$ Hz, 2H), 7.21 (d, $J = 7.9$ Hz, 2H), 4.62 (t, $J = 7.5$ Hz, 2H), 2.86 (t, $J = 7.3$ Hz, 2H), 2.33 (m, 2H), 2.24 (s, 3H).¹³C NMR (400MHz, D₂O, TMS) δ (ppm): 145.86, 144.28, 142.38, 139.51, 129.42, 128.37, 125.33, 59.86, 47.03, 26.12, 20.45. FI-IR (v/cm⁻¹): 3290, 3070, 2976, 1629, 1596, 1489, 1259, 1160. TG (N₂, 10 °C min⁻¹): T_d = 342°C.

Spectral data for IL5: ¹H NMR (400MHz, D₂O, TMS) δ (ppm): 2.69 (t, $J = 8.0$ Hz, 2H), 2.67 – 2.61 (m, 6H), 2.32 (t, $J = 7.0$ Hz, 2H), 1.53 – 1.39 (m, 2H), 0.62 (t, $J = 7.3$ Hz, 9H). ¹³C NMR (400MHz, D₂O, TMS) δ (ppm): 54.27, 52.26, 46.86, 16.79, 6.25. FI-IR (v/cm⁻¹): 3310, 2990, 1487, 1396, 1119, 1022. ESI-MS Positive Mass Peaks (m/z): 224.23, 447.44, 670.66; ESI-MS Negative Mass Peaks (m/z): 96.07. TG (N₂, 10 °C min⁻¹): T_d = 329°C.

Spectral data for IL6: ¹H NMR (400MHz, D₂O, TMS) δ (ppm): 3.14 (t, $J = 9.2$ Hz, 2H), 3.12 – 3.06 (m, 6H), 2.76 (t, $J = 7.1$ Hz, 2H), 1.97 – 1.86 (m, 2H), 1.07 (t, $J = 7.4$ Hz, 9H).¹³C NMR (400MHz, D₂O, TMS) δ (ppm): 54.61, 52.56, 47.14, 17.11, 6.47. FI-IR (v/cm⁻¹): 3329, 2989, 1478, 1332, 1171, 1104. ESI-MS Positive Mass Peaks (m/z): 224.21, 447.44; ESI-MS Negative Mass Peaks (m/z): 87.03. TG (N₂, 10 °C min⁻¹): T_d = 340°C.

Spectral data for IL7: ¹H NMR (400MHz, D₂O, TMS) δ (ppm): 3.16 – 3.12 (t, $J = 9.0$ Hz, 2H), 3.12 – 3.06 (m, 6H), 2.76 (t, $J = 7.0$ Hz, 2H), 1.98 – 1.85 (m, 2H), 1.07 (t, $J = 7.3$ Hz, 9H).¹³C NMR(400MHz, D₂O, TMS) δ (ppm): 54.59, 52.55, 47.12, 17.10, 6.50. FI-IR (v/cm⁻¹): 3295, 2989, 1487, 1396, 1119, 1022. ESI-MS Positive Mass Peaks (m/z): 224.29, 447.58; ESI-MS Negative Mass Peaks (m/z): 97.00. TG (N₂, 10 °C min⁻¹):

T_d = 337°C.

Spectral data for IL8: ^1H NMR(400MHz, D_2O , TMS) δ (ppm):7.33 – 7.27 (d, $J = 8.0$ Hz, 2H), 6.94 (d, $J = 8.0$ Hz, 2H), 2.87 – 2.81 (m, 2H), 2.76 (t, $J = 7.3$ Hz, 3H), 2.55 (t, $J = 7.0$ Hz, 2H), 1.96 (s, 3H), 1.66 (m, $J = 7.2$ Hz, 2H), 0.80 (t, $J = 7.3$ Hz, 9H). ^{13}C NMR (400 MHz, D_2O , TMS) δ (ppm): 141.99, 139.70, 129.25, 125.17, 54.44, 52.37, 47.00, 20.30, 16.97, 6.37. FI-IR (v/cm^{-1}): 3299, 2987, 1599, 1486, 1396, 1249, 1121, 1026, 1002. TG (N_2 , $10\text{ }^\circ\text{C min}^{-1}$): $T_d = 339^\circ\text{C}$.

Spectral data for IL9: ^1H NMR (400 MHz, D_2O , TMS) δ (ppm) 8.54 (s, 1H), 7.26 (d, $J = 1.7$ Hz, 2H), 4.06 (t, $J = 7.2$ Hz, 4H), 2.63 (t, $J = 7.5$ Hz, 4H), 2.01 (m, 4H). ^{13}C NMR (400 MHz, D_2O , TMS) δ (ppm) 135.50 , 122.42 , 47.71 , 47.10 , 24.83 . FI-IR (v/cm^{-1}): 3342, 3041, 2987, 1599, 1486, 1396, 1249, 1121, 1026, 1002. TG (N_2 , $10\text{ }^\circ\text{C min}^{-1}$): $T_d = 326^\circ\text{C}$.

For example, the NMR spectrum of IL4

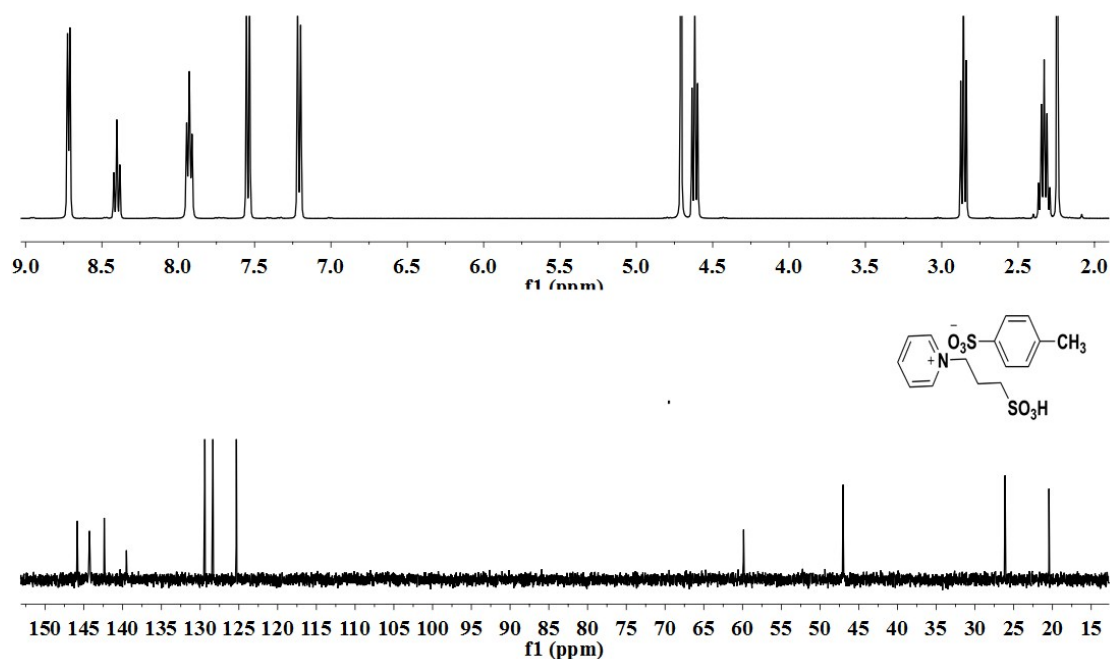


Fig. 1 IL4 in ^1H NMR and ^{13}C NMR

1.3 Acidity characterization of ionic liquids

The SO_3H -functionalized acidic ILs were dissolved in distilled water, and 4-nitroaniline ($\text{pK}_a = 0.99$) was added as indicator. Their UV-vis spectra were recorded on a UV (HP-8453) spectrophotometer at room temperature. The acidity of the different concentration of IL1 was examined using 4-nitroaniline as indicator in H_2O and the results are shown in Fig. 2. We observed that the maximum absorbance of

unprotonated 4-nitroaniline is at 382 nm in H₂O. As the acid concentration of IL1 increases, the absorbance of the unprotonated form of the 4-nitroaniline observed at 382 nm decreases.

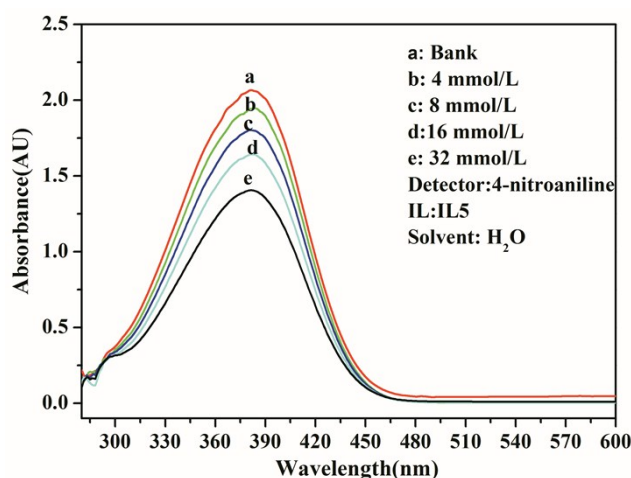
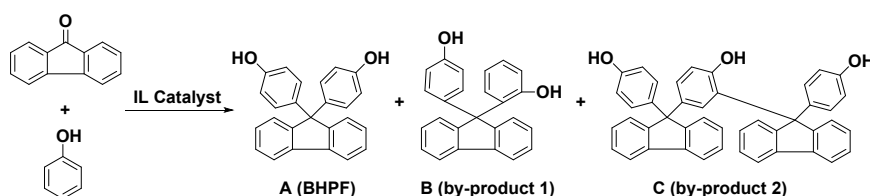


Fig. 2 Absorption spectra of 4-nitroaniline for various concentration of IL1 in H₂O

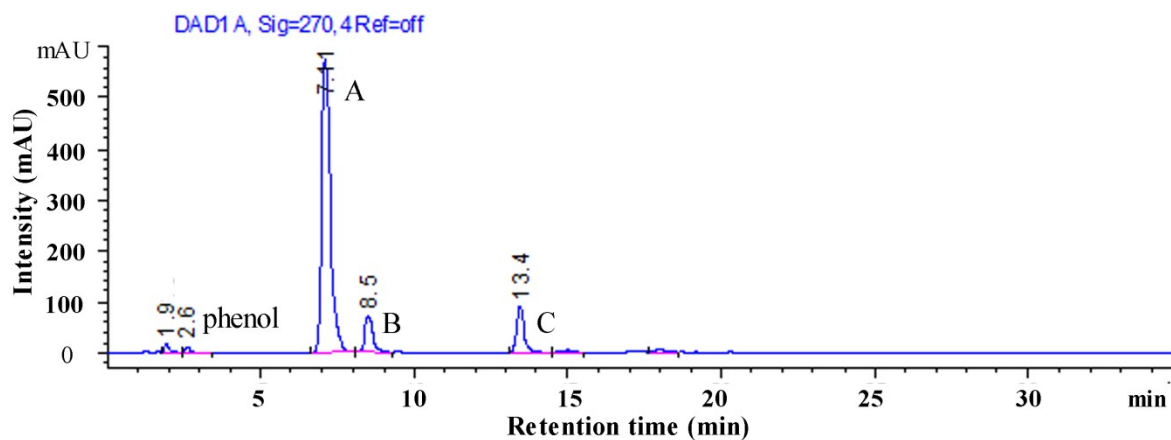
2. The qualitative analysis of the catalytic reaction



Scheme 3 The 9-fluorenone condensation with phenol

The crude product was qualitatively analyzed by High Performance Liquid Chromatography / Mass Selective (LC / MS) (Agilent 1100 / 6130)

The results of LC-MS analysis clarified that there were three products depicted as compounds A-C generating in reaction process. The spectrum is shown in Figure 3.



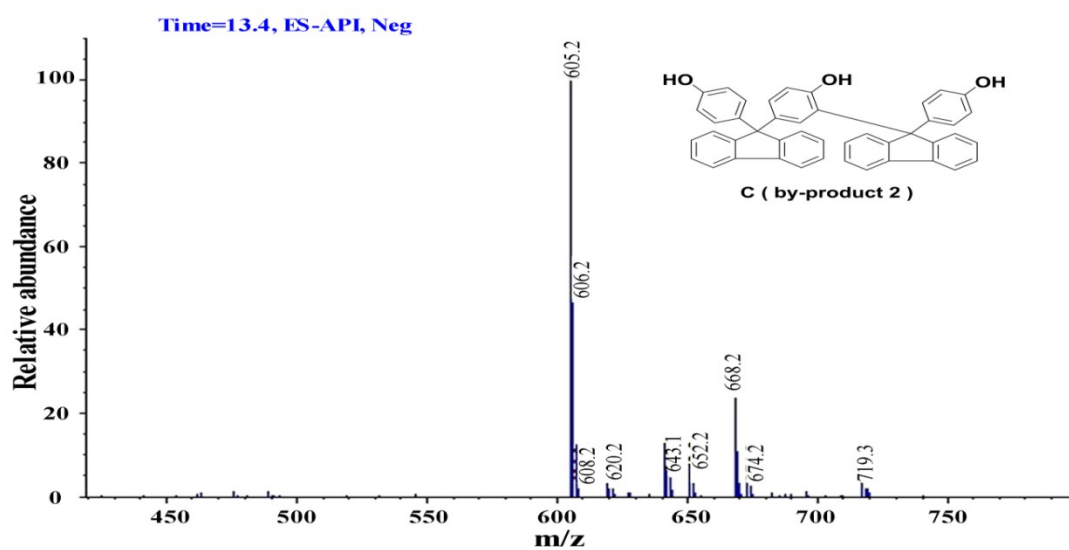
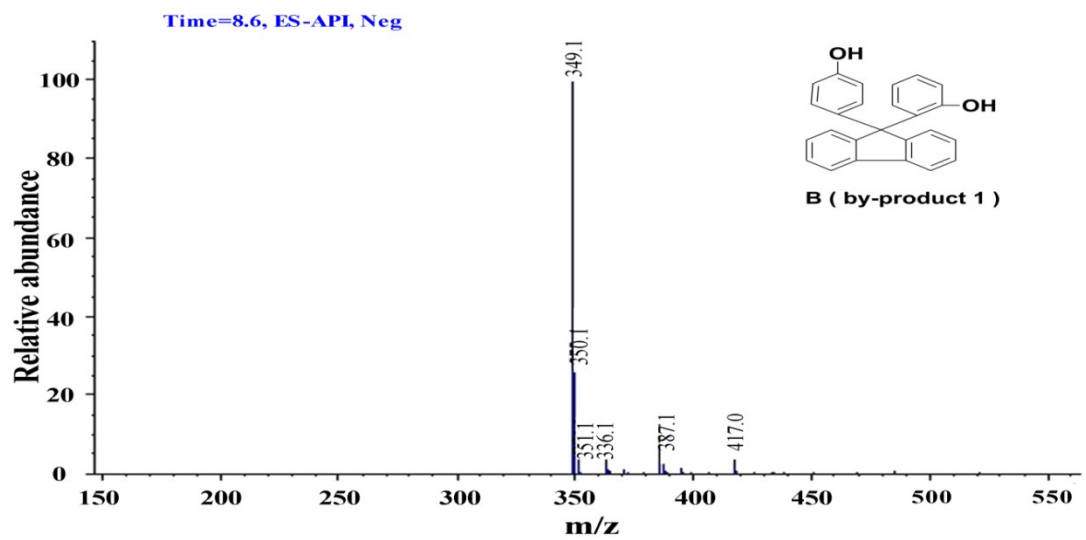
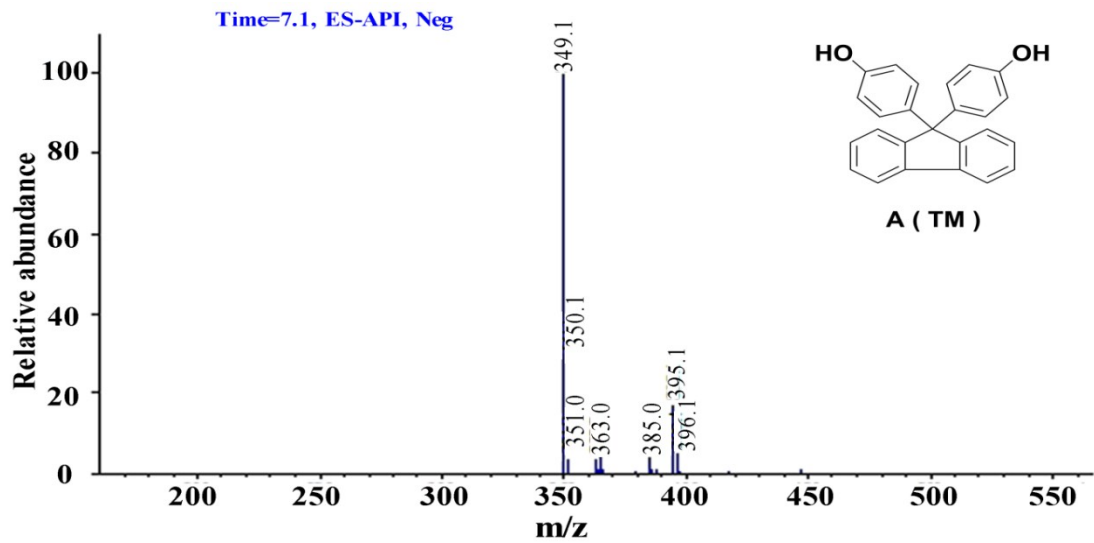


Fig. 3 LC / MS of crude product

In the condensation reaction of 9-fluorenone with phenol, The NMR spectrum of the three products A, B and C are shown in Figure 4, Figure 5, Figure 6.

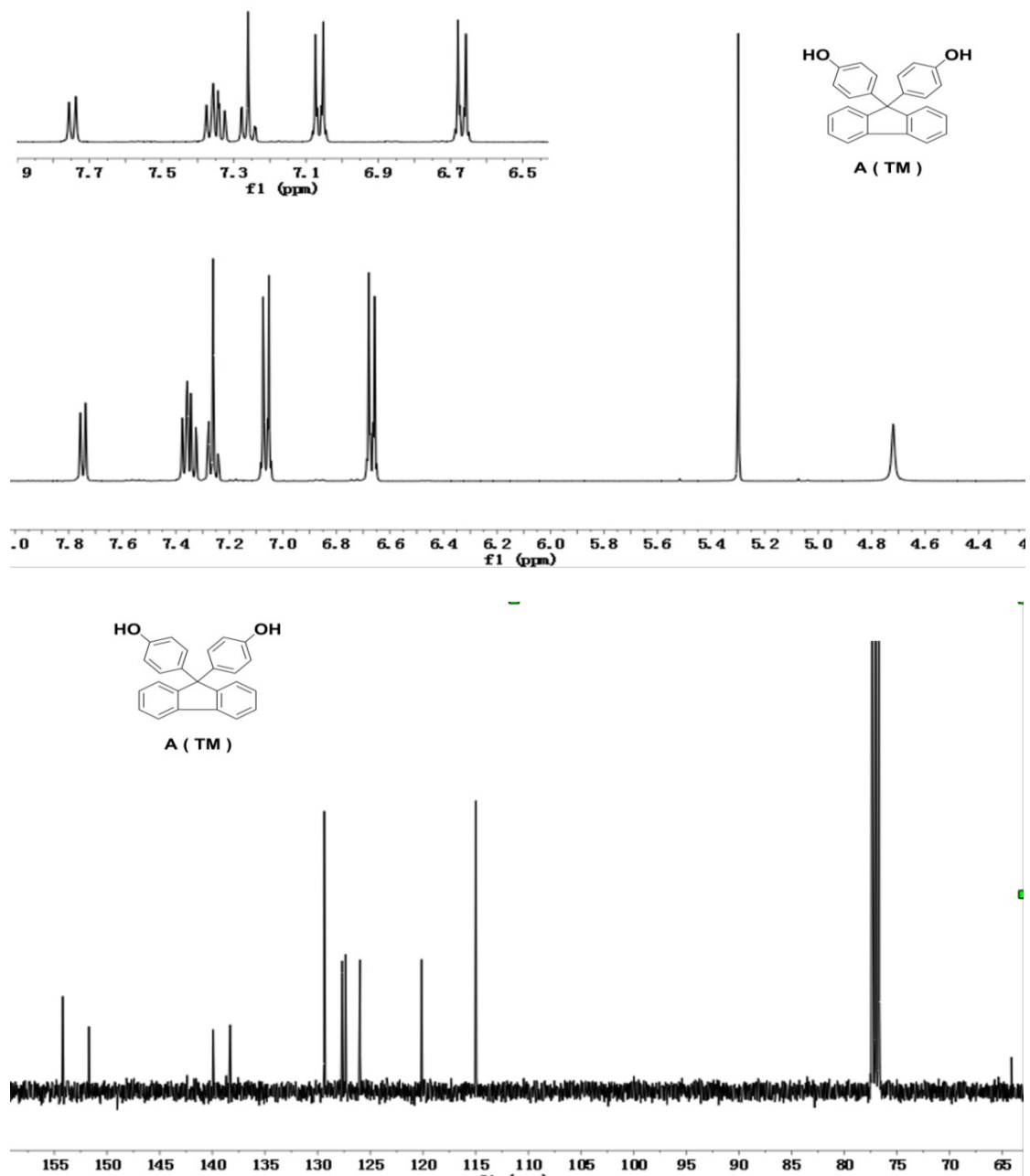


Fig. 4 A in ^1H NMR and ^{13}C NMR

^1H NMR (400 MHz, CDCl_3 , TMS) δ (ppm): 7.39 – 7.31 (t, $J = 7.5$ Hz, 4H), 7.30 – 7.23 (t, $J = 7.3$ Hz, 2H), 7.09 – 7.03 (d, $J = 7.1$ Hz, 4H), 6.70 – 6.64 (d, $J = 7.1$ Hz, 4H), 5.30 (s, 2H). ^{13}C NMR (400 MHz, CDCl_3 , TMS) δ (ppm): 154.19, 151.71, 139.93, 138.30, 129.37, 127.68, 127.34, 125.98, 120.13, 114.98.

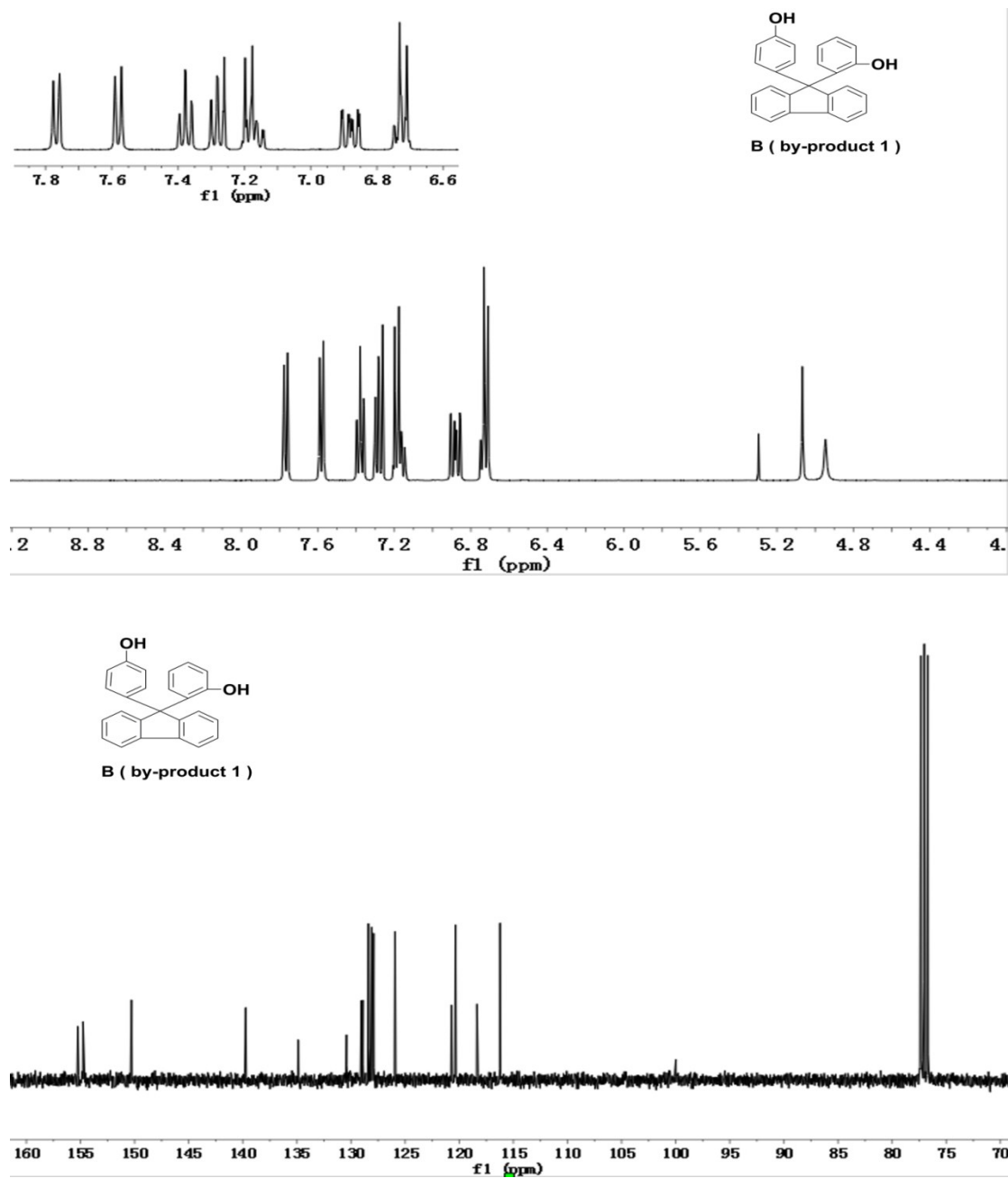


Fig. 5 B in ¹H NMR and ¹³C NMR

¹H NMR (400 MHz, CDCl₃, TMS) δ (ppm): 7.77 (d, $J = 7.4$ Hz, 2H), 7.58 (d, $J = 7.4$ Hz, 2H), 7.38 (t, $J = 7.5$ Hz, 2H), 7.32 (d, $J = 7.5$ Hz, 1H), 7.20 (t, $J = 7.5$ Hz, 2H), 7.15 – 7.13 (d, $J = 7.4$ Hz, 2H), 6.88 (t, $J = 7.5$ Hz, 1H), 6.76 (t, $J = 7.5$ Hz, 1H), 6.71 – 6.67 (d, $J = 7.3$ Hz, 2H), 6.75 (d, $J = 7.5$ Hz, 1H), 5.07 (s, 1H), 4.95 (s, 1H). ¹³C NMR (400MHz, CDCl₃, TMS) δ (ppm): 155.25, 154.77, 150.29, 139.73, 134.88, 130.42, 129.06, 128.91, 128.40, 128.09, 127.91, 125.93, 120.72, 120.35, 118.36, 116.22.

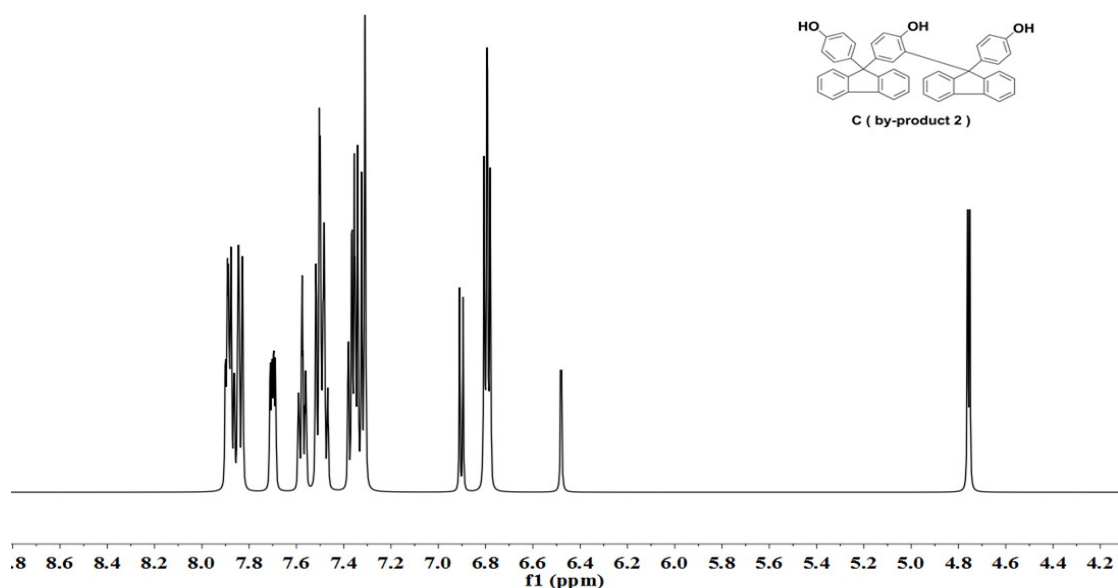


Fig. 6 C in ^1H NMR

^1H NMR (400 MHz, CDCl_3 , TMS) δ (ppm): 7.91 (d, $J = 7.5\text{Hz}$, 1H), 7.88 (d, $J = 7.6\text{ Hz}$, 2H), 7.87 – 7.85 (m, 1H), 7.85 – 7.82 (m, 2H), 7.70 (t, $J = 7.3\text{Hz}$, 2H), 7.58 (t, $J = 7.6\text{Hz}$, 2H), 7.52 (d, $J = 2.2\text{ Hz}$, 1H), 7.50 (t, $J = 2.1\text{ Hz}$, 2H), 7.48 (t, $J = 7.5\text{ Hz}$, 2H), 7.37 (t, $J = 7.5\text{Hz}$, 2H), 7.36 – 7.31 (m, 4H), 7.31 (d, $J = 2.0\text{ Hz}$, 1H), 6.89 (d, $J = 7.4\text{ Hz}$, 1H), 6.82 – 6.76 (m, 4H), 6.44 (s, 1H), 4.76 (s, 2H).

Based on the above LC-MS and NMR spectra, we can determine the specific structure of the 9-fluorenone and phenol condensation products A (BHPF), B (by-product 1) and C (by-product 2).

3. The quantitative analysis of the catalytic reaction

The reaction was quantitatively analyzed by High Performance Liquid Chromatography (HPLC 1100).

The performance of the catalysts is characterized quantitatively by the conversion of 9-fluorenone (Con %), and the selectivity to A, B or C obtained at the optimized conditions.

Conversion of 9-fluorenone is calculated as follows:

$$\text{Con (\%)} = [m(9\text{-fluorenone})_I - m(9\text{-fluorenone})_T] / m(9\text{-fluorenone})_I \times 100,$$

where $m(9\text{-fluorenone})_I$ and $m(9\text{-fluorenone})_T$ are the mass of 9-fluorenone at initial and terminal reaction time

Selectivity is calculated as follows:

$$\text{Sel\%} = N_A / [N_A + N_B + N_C] \times 100,$$

where N_A , N_B or N_C is the number of moles of A, B or C

The catalytic reactions were analyzed by HPLC on a HP1100 series instrument and detection was carried out at 257nm and 275 nm. The maximum absorption wavelength of 9-fluorenone is 257 nm, while the maximum absorption wavelength of products A, B, and C is 275 nm. So, the conversion of 9-fluorenone was quantified using a DAD detector with an absorption wavelength of 257 nm based on a 9-fluorenone-based standardized calibration curve, and the product selectivity was calculated by an area normalization method using a DAD detector having an absorption wavelength of 275 nm. Shown below in Figure 7 is HPLC of 9-fluorenone. Figures 8 and 9 show typical HPLC of the same reaction solution at different wavelengths in the condensation reaction of 9-fluorenone and phenol. Among them, the peak at 6.0 minutes is phenol, 15.6 min is 9-fluorenone, 18.1 minutes is A (TM), 21.0 minutes is B (by-product 1) and 23.9 minutes is C (by-product 2).

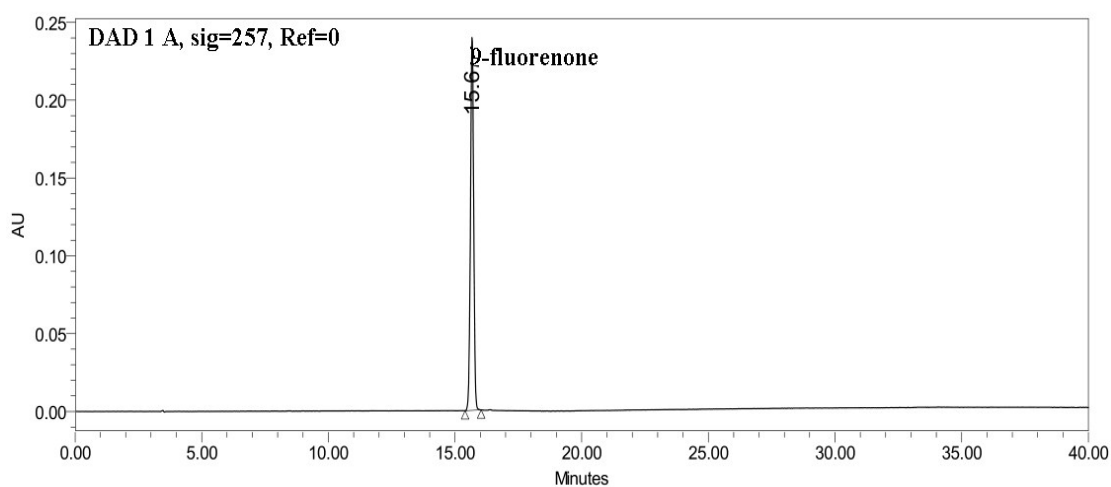


Fig. 7 HPLC of 9-fluorenone

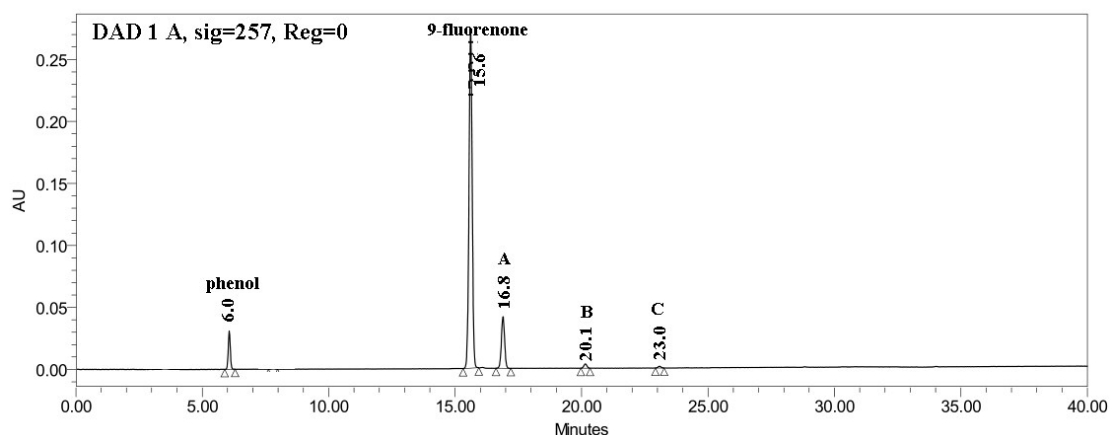


Fig. 8 HPLC of reaction liquid at 257nm

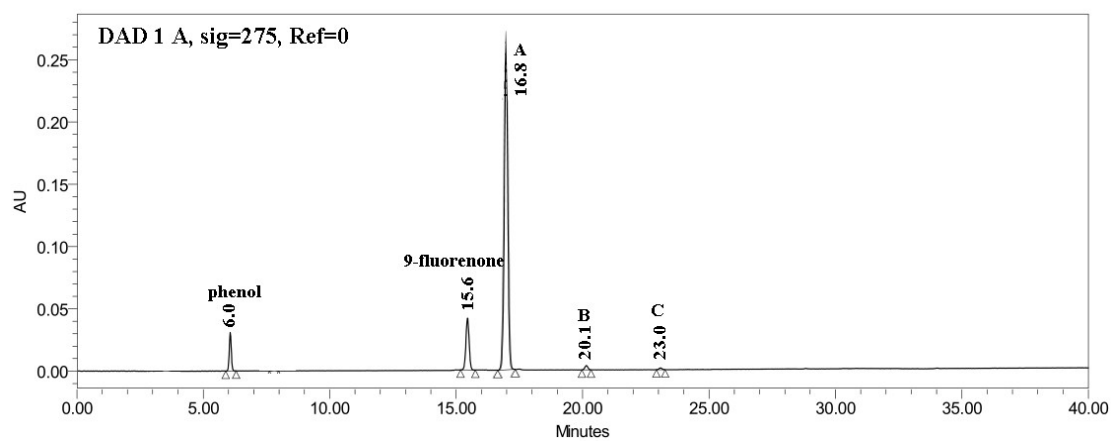


Fig. 9 HPLC of reaction liquid at 275nm